

# Tailor-Made pH-Responsive Poly(choline phosphate) Prodrug as a Drug Delivery System for Rapid Cellular Internalization

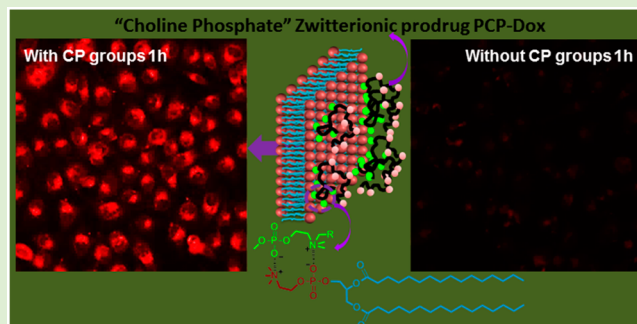
Wenliang Wang,<sup>†,‡,§</sup> Bo Wang,<sup>†,§</sup> Xiaojing Ma,<sup>\*,†</sup> Sanrong Liu,<sup>†</sup> Xudong Shang,<sup>†</sup> and Xifei Yu<sup>\*,†,‡</sup>

<sup>†</sup>The Polymer Composites Engineering Laboratory, Changchun Institute of Applied Chemistry, Chinese Academy of Sciences, Changchun 130022, People's Republic of China

<sup>‡</sup>University of Chinese Academy of Sciences, Beijing 100049, People's Republic of China

## Supporting Information

**ABSTRACT:** Rapid cellular uptake and efficient drug release in tumor cells are two of the major challenges for cancer therapy. Herein, we designed and synthesized a novel pH-responsive polymer–drug conjugate system poly(2-(methacryloyloxy)ethyl choline phosphate)-*b*-poly(2-methoxy-2-oxoethyl methacrylate-hydrazide-doxorubicin) (PCP-Dox) to overcome these two challenges simultaneously. It has been proved that PCP-Dox can be easily and rapidly internalized by various cancer cells due to the strong interaction between multivalent choline phosphate (CP) groups and cell membranes. Furthermore, Dox, linked to the polymer carrier via acid-labile hydrazone bond, can be released from carriers due to the increased acidity in lysosome/endosome (pH 5.0–5.5) after the polymer prodrug was internalized into the cancer cells. The cell viability assay demonstrated that this novel polymer prodrug has shown enhanced cytotoxicity in various cancer cells, indicating its great potential as a new drug delivery system for cancer therapy.



## 1. INTRODUCTION

Chemotherapy is one of the main approaches in cancer therapy that parallels to surgery and radiotherapy. However, the clinical utilization of conventional chemotherapy drugs like doxorubicin (Dox) is limited by their short half-time and severe toxicity to normal tissues.<sup>1</sup> In the past decades, various drug delivery systems, such as polymer–drug conjugates (prodrugs),<sup>2–8</sup> nanomicelles,<sup>9,10</sup> nanogels,<sup>11,12</sup> and polymersomes,<sup>13</sup> have been designed as a most promising platform to overcome these problems. Among these delivery systems, prodrugs in which anticancer drugs are covalently conjugated to the polymer molecules via cleavable hydrazone,<sup>5,14</sup> esters,<sup>15</sup> disulfide,<sup>16</sup> or other biologically responsive bonds<sup>17</sup> have attracted tremendous interest. Prodrug exhibits some unique advantages, for example, they can improve pharmacokinetics, control drug release and circumvent the drug efflux pumps, namely, P-glycoprotein and multidrug resistance-associated protein,<sup>18,19</sup> suggesting their great potential for application as an effective anticancer drug delivery system.

Although the polymer prodrug provides a prospective platform in the fight against cancer, the sluggish and poor cellular internalization of the prodrug limits the dosages of anticancer drugs to the level below therapeutic window and severely hampers the efficacy of cancer therapy, especially for the cargo molecules like nucleic acids, peptides, or proteins, which are difficult to enter into cells and unstable in physiological conditions.<sup>20</sup> To address the challenges, few studies have been particularly focused on how to improve the

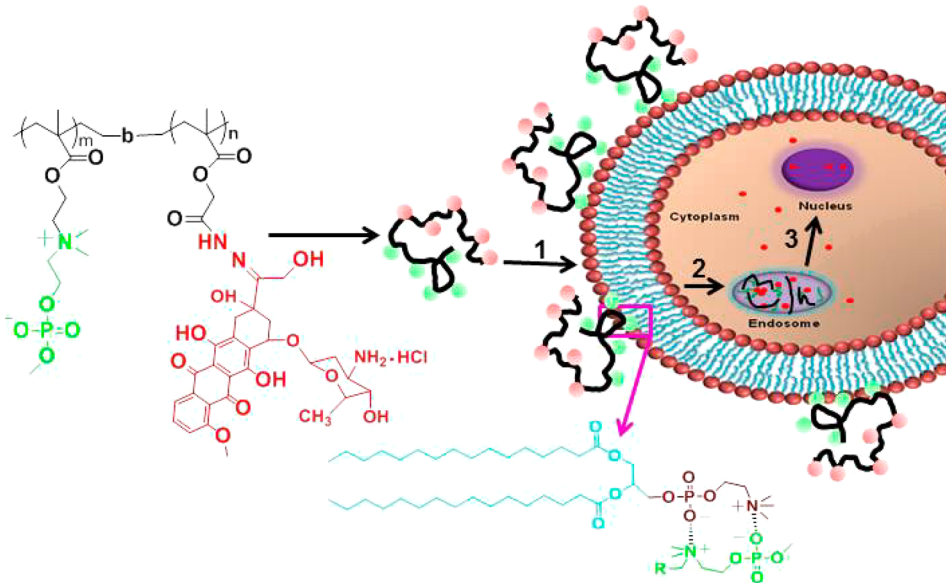
cellular internalization efficiency. For example, Du et al. reported that they prepared a novel nanoparticle to improve cellular internalization by reversing the surface charge from negative to positive according to spatial variations in tumor extracellular pH values, which showed enhanced cytotoxicity in drug-resistant cancer stem cells.<sup>21</sup> In addition, it has been found that modification of the polymer carriers with targeting ligands contribute to improve the cellular internalization efficiency.<sup>3,22,23</sup> However, this improvement is the consequent results of the specific targeted ligands and receptors, and this targeted ligands and receptors interactions can only be applied to one or several specific tumor cells, which limit its extensive application.

In our previous works, we have designed and synthesized a bioinspired functional group choline phosphate (CP), which shows phosphatidyl choline groups (PC, headgroup of phospholipids in all eukaryotic cell membranes) orientated opposite to what they are on cell membranes.<sup>24</sup> It has been found that the polymers decorated with multivalent CP groups could strongly bind to cell membranes and then rapidly taken up by nucleated cells, where such strong adhesion is mediated by quadrupole interaction between the multivalent CP and PC groups.<sup>25–28</sup> In addition, Hu et al. have recently detailed the synthesis of choline phosphate methacrylates and

Received: March 28, 2016

Revised: April 29, 2016

Published: May 5, 2016

**Scheme 1.** Schematic Illustration of the Prodrug PCP-Dox Cellular Internalization and Its Intracellular Drug Release

functional choline phosphate polymers that have been applied as prodrugs, hydrogels, and other derivatives.<sup>29,30</sup> Wang et al. also reported a stable  $TiO_2$ /lipid interface with DPCP, which represented the first example of CP liposome applied in metal oxides;<sup>31</sup> what's more, Chen et al. designed a CP-modified surface to resist protein adsorption but promote cell adhesion simultaneously,<sup>32</sup> which indicated the CP groups have great potential to be a biomedical material. Based on these results, we proposed to design and synthesize a novel kind of polymer drug delivery system modified with CP groups, which can not only be used to promote the cellular internalization of anticancer drugs, but also be applied to various tumor cells.

As a proof-of-concept, we synthesized a novel endosomal pH-sensitive prodrug PCP-Dox (Scheme 1) at the first time. Dox has been conjugated to a macromolecular carrier via an acid-labile hydrazone bond, which is sufficiently stable at pH 7.4 but readily cleavable in an acidic environment such as in endosome/lysosome. Dox is not only a vigorous drug for various cancer cell approved by FDA,<sup>33</sup> but also acts as a fluorescent reporter for our drug delivery system. The location and efficiency of prodrug internalized into the cells can be real-time monitored by detecting the fluorescence distribution and intensity of Dox in cells. When the prodrug arrived at the tumor cells, it will bind to the cell membrane easily and rapidly with PC headgroups via multiple CP-PC quadrupole interaction (1, Scheme 1), and then internalize into the cell (2, Scheme 1). After the prodrug was internalized by tumor cells, the hydrazone bond will be continuously cleaved at lysosome/endosome pH environment and the Dox could escape from the lysosome/endosome, then diffuse into nucleus and lead to DNA double-strand breaks and inhibition of DNA replication and transcription (3, Scheme 1),<sup>8,34</sup> killed the tumor cells finally.

## 2. EXPERIMENTAL SECTION

**2.1. Materials.** The ATRP initiator of 3-azidopropyl 2-bromo-2-methylpropanoate was synthesized according to previous report.<sup>35</sup> 2-Chloro-2-oxo-1,3,2-dioxaphospholane was purchased from Aladdin. Methyl glycolate, methacryloyl chloride, 2-(dimethylamino) ethyl methacrylate, butylated hydroxytoluene, hydrazine hydrate (50%), trifluoroacetic acid, and doxorubicin hydrochloride (Dox-HCl) were

purchased from Sigma-Aldrich. All chemicals were used without further purification unless otherwise mentioned.

**2.2. Characterization.** NMR spectra were recorded by Unity-400 NMR spectrometer at room temperature and the MS spectra were measured by Bruker micoTOF-QII. The size distribution of the prodrug PCP-Dox was determined by dynamic light scattering (DLS) using a Zetasizer Nano-ZS from Malvern Instruments with He-Ne laser. The measurements were made with wavelength of 633 nm at 25 °C and angle detection at 173°. Polydispersity and molecular weights of the polymers PMEMA-Br were determined by gel permeation chromatography (GPC, Waters 1525) setup comprising Agilent PL gel 5 μm MIXED-C columns using Waters 2414 refractive index detector. THF was eluent with the flow rate was 1.0 mL/min at 35 °C, and series of polystyrene were used as standards for calibration curve. The fluorescence images were obtained by confocal laser scanning microscopy (CLSM, LSM 700 Carl Zeiss Microscopy). The Dox content of the prodrug was determined by UV-vis spectroscopy (NanoDrop 2000c from Thermo Scientific). The cell viability was detected by synergy microplate reader using a Synergy H1Microplate Reader from BioTek. The fluorescence intensity internalized into the cells at fixed time interval was measured by flow cytometry (FACS, Guava easyCyte 6–2L from Millipore), the excitation and emission were set at 480 and 560 nm.

**2.3. Synthesis of 2-(Methacryloyloxy) Ethyl Choline Phosphate, MCP.** MCP was synthesized based on our previous synthetic method.<sup>28</sup> All glassware were flame dried and protected by argon before using. Briefly, methanol (1.92 g, 0.06 mol) prepared by distilling sodium methoxide methanol solution, 2-(dimethylamino)ethyl methacrylate (18.87 g, 0.12 mol) dried by  $CaH_2$ , acetonitrile (60 mL) dried by  $CaH_2$  and distilled freshly before using, and butylated hydroxytoluene (250 mg) were added to a 100 mL Schlenk flask. The mixed solution was stirred and cooled to -78 °C. Subsequently, 2-chloro-2-oxo-1,3,2-dioxaphospholane (7.12 g, 0.05 mol) was added dropwise about 2 h. The reaction was removed to room temperature for another 4 h. After that, the reaction was cooled to -20 °C to filter off the precipitate, the filtrate was directly removed to a Schlenk flask, the whole process was operated under argon atmosphere. Finally, the resulting solution was stirred another 12 h at 70 °C, after cooled to room temperature, the resulting solution was precipitated into tetrahydrofuran with three times. The precipitate was dried under reduced pressure (yield: 52%).  $^1H$  NMR (400 MHz,  $D_2O$ ): Figure 1a,  $\delta$  (ppm) 6.16 and 5.72 (s, -OC(CH<sub>3</sub>)=CH<sub>2</sub>), 4.63 (t, -CH<sub>2</sub>O-CO-), 3.90 (t, -CH<sub>2</sub>OP), 3.78–3.71 (m, -CH<sub>2</sub>N(CH<sub>3</sub>)<sub>2</sub>-CH<sub>2</sub>-), 3.60–3.57 (d, P-OCH<sub>3</sub>), 3.24 (s, -N-(CH<sub>3</sub>)<sub>2</sub>), 1.97 (s, -OC(CH<sub>3</sub>)=CH<sub>2</sub>);  $^{31}P$  NMR (400 MHz,  $CD_3OD$ ):  $\delta$  (ppm) 0.96 (s); and  $^1H$  NMR (400 MHz,

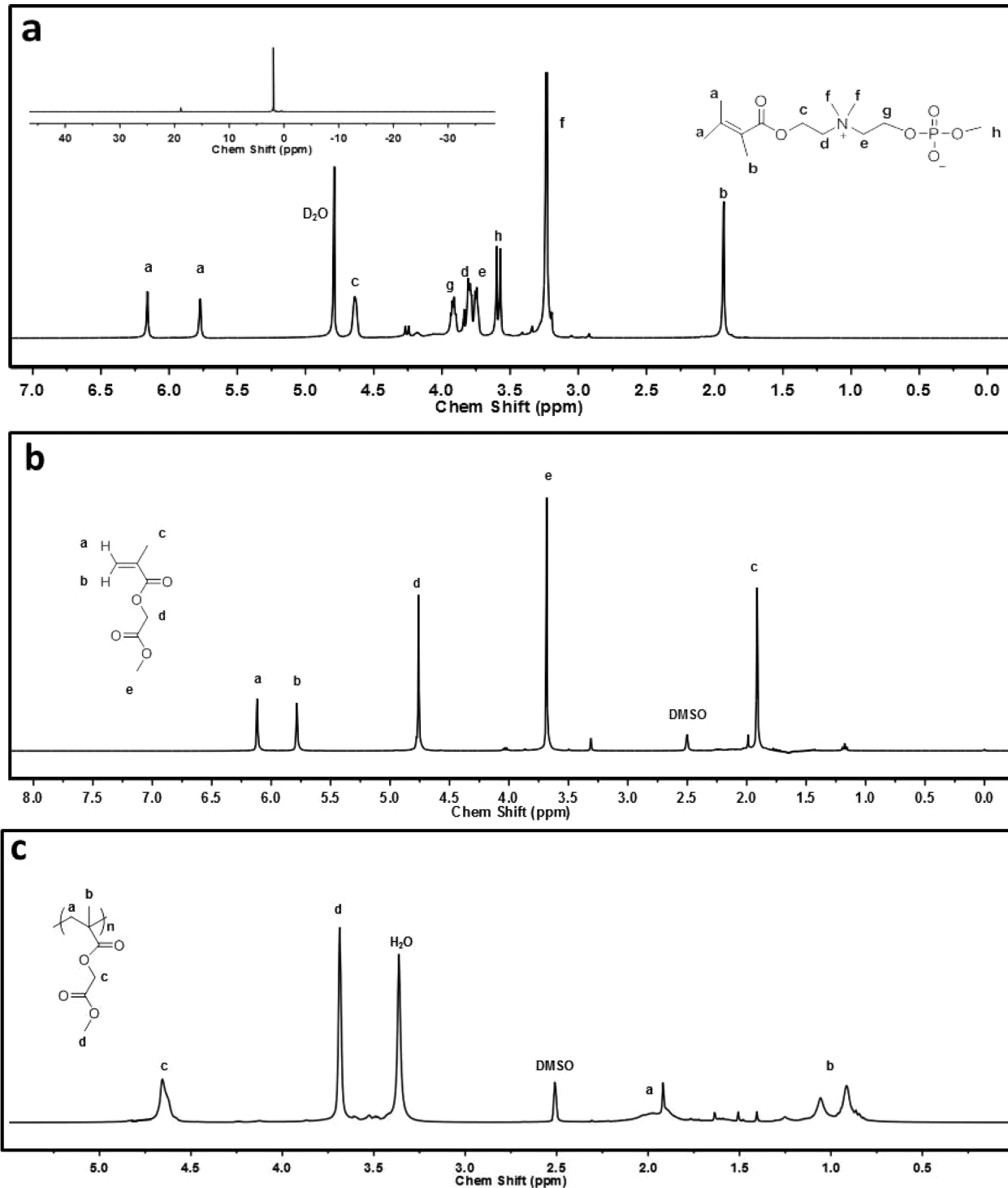


**Figure 1.** (a) <sup>1</sup>H and <sup>31</sup>P NMR spectra of MCP; (b) <sup>1</sup>H NMR spectrum of MEMA; (c) <sup>1</sup>H NMR spectra of PMEMA.

DMSO-*d*<sub>6</sub> and CD<sub>3</sub>OD, 1:1, v/v): Figure S1,  $\delta$  (ppm) 6.06 and 5.66 (s, -OC(CH<sub>3</sub>)=CH<sub>2</sub>), 4.51 (t, -CH<sub>2</sub>O-CO-), 3.52 (t, -CH<sub>2</sub>OP), 3.74–3.65 (m, -CH<sub>2</sub>N(CH<sub>3</sub>)<sub>2</sub>-CH<sub>2</sub>), 3.42–3.39 (d, CH<sub>3</sub>OP), 3.13 (s, -N-(CH<sub>3</sub>)<sub>2</sub>), 1.87 (s, -OC(CH<sub>3</sub>)=CH<sub>2</sub>).

**2.4. Synthesis of 2-Methoxy-2-oxoethyl Methacrylate, MEMA.** MEMA was synthesized according to previous report.<sup>36</sup> In brief, methyl glycolate (5.41 g, 0.06 mol), triethylamine (6.7 g, 0.066 mol), and methylene dichloride (100 mL) were added to a flask at 0 °C. Then methacryloyl chloride (6.27 g, 0.06 mol) was added dropwise, after 2 h, the reaction was removed to room temperature and stirred another 20 h. Then the solid was filtered off and the filtrate

was concentrated under rotary evaporation. The crude product was purified by silica gel column chromatography (yield: 78.7%). <sup>1</sup>H NMR (400 MHz, DMSO-*d*<sub>6</sub>): Figure 1b,  $\delta$  (ppm) 6.1 and 5.8 (s, -OC(CH<sub>3</sub>)=CH<sub>2</sub>), 4.8 (s, -CH<sub>2</sub>O-CO), 3.7 (s, -OCH<sub>3</sub>), 1.9 (s, -OC(CH<sub>3</sub>)=CH<sub>2</sub>).

**2.5. Synthesis of Poly(2-methoxy-2-oxoethyl methacrylate), PMEMA.** PMEMA was synthesized by atom transfer radical polymerization (ATRP). ATRP initiator of 3-azidopropyl 2-bromo-2-methylpropanoate (50 mg, 0.2 mmol), 2,2'-dipyridyl (bpy, 62.4 mg, 0.4 mmol), MEMA (0.469 g, 3.0 mmol), and THF (5 mL) were added to a 25 mL Schlenk flask under argon atmosphere, which was then put

through three cycles of freeze–pump–thaw with argon prior to added CuBr (28.6 mg, 0.2 mmol). The mixture was stirred at room temperature for 24 h. The polymerization was stopped by exposing the mixture to air. The solution was diluted with THF and passed through neutral alumina column. The resulting solution was concentrated under reduced pressure, and then precipitated into excess methanol. The precipitate was dried under vacuum (yield: 75%). <sup>1</sup>H NMR (400 MHz, DMSO-*d*<sub>6</sub>): Figure 1c, δ (ppm) 4.66 (s, -OC-OCH<sub>2</sub>CO-), 3.69 (s, -OCH<sub>3</sub>), 2.0 (s, -CCH<sub>2</sub>C-), 1.06–0.91 (d, -CCH<sub>3</sub>).

### 2.6. Synthesis of Poly(2-(methacryloyloxy) ethyl choline phosphate)-*b*-Poly(2-methoxy-2-oxoethyl methacrylate), PCP-*b*-PMEMA. PMEMA<sub>12</sub> (Table 1, 2#, 0.20 g, 0.1 mmol),

**Table 1.** PDI and *M<sub>n</sub>* of Polymers Synthesized by ATRP

entries	polymers	target <i>D<sub>p</sub></i>	<i>M<sub>n</sub></i> <sup>a</sup> g·mol <sup>-1</sup>	<i>M<sub>n</sub></i> <sup>b</sup> g·mol <sup>-1</sup>	PDI <sup>a</sup>
1	PMEMA <sub>30</sub> -Br	30	5179	4990	1.37
2	PMEMA <sub>12</sub> -Br	15	2065	2146	1.36
3	PCP- <i>b</i> -PMEMA <sub>12</sub>		n/a	13946	n/a
4	PCP- <i>b</i> -PMEMA <sub>30</sub>		n/a	19150	n/a

<sup>a</sup>Measured by GPC (THF, PS standards). <sup>b</sup>Calculated on the basis of <sup>1</sup>HMR spectrum.

MCP (1.77 g, 6 mmol), bpy (31.2 mg, 0.2 mmol), and a mixed solvent of methanol and THF (7 mL, 3:4, v/v) was added to a 25 mL Schlenk flask and put through three cycles of freeze–pump–thaw with argon and then added CuBr (14.3 mg, 0.1 mmol). The reaction was processed at room temperature for 48 h and stopped by exposing the solution to air. Finally, the excessive MCP and catalyst was removed by dialysis bag with MWCO 2000 membrane. After freeze-drying, PCP-*b*-PMEMA<sub>12</sub> (Table 1, 3#) was collected with yield 46.6%. <sup>1</sup>H NMR (400 MHz, DMSO-*d*<sub>6</sub> and CD<sub>3</sub>OD, 1:1, v/v): Figure 2a, δ (ppm) 4.59 (s, -COCH<sub>2</sub>O-CO-), 4.36 (s, -CH<sub>2</sub>O-CO-), 3.75 (m, -CH<sub>2</sub>N(CH<sub>3</sub>)<sub>2</sub>-CH<sub>2</sub>), 3.67 (s, -OCH<sub>3</sub>), 3.54 (t, -POCH<sub>2</sub>-), 3.44–3.42 (d, -POCH<sub>3</sub>), 3.23 (s, -N-(CH<sub>3</sub>)<sub>2</sub>), 1.88 (s, -CCH<sub>2</sub>C-), 1.09–0.93 (d, -CCH<sub>3</sub>); and <sup>31</sup>P NMR (400 MHz, DMSO-*d*<sub>6</sub> and CD<sub>3</sub>OD): δ (ppm) 0.96 (s).

**2.7. Synthesis of Poly(2-methoxy-2-oxoethyl methacrylate)-Hydrazide-Dox, PMEMA-Hyd-Dox.** PMEMA<sub>30</sub> (Table 1, 2#, 0.1 g) was dissolved in the mixed solvent DMF and methanol (5 mL, 3:2, v/v), and hydrazine hydrate (0.2 mL) was then added to the mixture. The mixture was stirred overnight at room temperature. Then, the mixture was precipitated into excessive methanol, and the precipitate was dried under vacuum. <sup>1</sup>H NMR (400 MHz, DMSO-*d*<sub>6</sub>): δ (ppm) 9.28 (s, H<sub>2</sub>N-HN-OC-), 4.38 (s, -HN-OC-OCH<sub>2</sub>CO-), 1.92 (s, -CCH<sub>2</sub>C-), 0.81–1.00 (d, -CCH<sub>3</sub>).

PMEMA<sub>30</sub>-hydrazide (30 mg) was dissolved in the mixed solvent DMF and methanol (5 mL, 3:2, v/v), and doxorubicin hydrochloride (10 mg) and trifluoroacetic acid (5 μL) were added to the mixture. The mixture was stirred at room temperature for 48 h in the dark. Then, the mixture was dialyzed against deionized water (MWCO 3500) for 2 days and lyophilized with a yield of 70.5%.

**2.8. Synthesis of Poly(2-(methacryloyloxy) ethyl choline phosphate)-*b*-Poly(2-methoxy-2-oxoethyl methacrylate)-Hydrazide, PCP-*b*-PMEMA-Hydrazide.** PCP-*b*-PMEMA<sub>12</sub> (Table 1, 3#, 0.10g) and hydrazine hydrate (60 μL) were added to the mixture of dimethylformamide (DMF, 3 mL) and methanol (2 mL) into a 25 mL flask. The mixture was stirred overnight at room temperature, and the resulting solution was dialyzed against deionized water (MWCO 2000) for 24 h and lyophilized with a yield of 85%. <sup>1</sup>H NMR (400 MHz, DMSO-*d*<sub>6</sub> and CD<sub>3</sub>OD, 1:1, v/v): Figure 2b, δ (ppm) 4.36 (s, -CH<sub>2</sub>OCO-), 3.75 (m, -CH<sub>2</sub>N(CH<sub>3</sub>)<sub>2</sub>-CH<sub>2</sub>), 3.54 (t, -CH<sub>2</sub>OP), 3.44–3.42 (d, -POCH<sub>3</sub>), 3.24 (s, -N(CH<sub>3</sub>)<sub>2</sub>), 1.88 (s, -CCH<sub>2</sub>C-), 1.09–0.94 (d, -CCH<sub>3</sub>); <sup>31</sup>P NMR (400 MHz, DMSO-*d*<sub>6</sub> and CD<sub>3</sub>OD): δ (ppm) 0.96 (s).

**2.9. Synthesis of the Polymer Prodrug, PCP-Dox.** PCP-*b*-PMEMA<sub>12</sub>-Hydrazide (40 mg), doxorubicin hydrochloride (15 mg),

trifluoroacetic acid (5 μL), and the mixed solvent of DMF (3 mL) and methanol (2 mL) was added to a 25 mL flask. The mixture was reacted in the dark at room temperature for 2 days. The resulting solution was dialyzed against distilled water (MWCO 3500) for 48 h and lyophilized with a yield of 86.5%.

**2.10. Determining the Percent Dox of PCP-Dox and PMEMA-Hyd-Dox via UV–Vis Spectroscopy.** The loading amount of Dox was determined via UV–visible absorption spectra. A total of 2 mg of PCP-Dox and 2 mg of PMEMA-Hyd-Dox were treated with 1 N HCl (0.5 mL) for 24 h, respectively, and then the solution was diluted to 10 mL with DI water. Finally, the absorbance intensity of PCP-Dox and PMEMA-Hyd-Dox diluted solution was determined by UV–vis spectroscopy at 480 nm for Dox. The experiment was performed in quintuplicate, and then the Dox content was calculated via the calibration curve of free Dox (shown in Figure S7 in SI).

**2.11. Preparation of the PCP-Dox Prodrug and PMEMA-Hyd-Dox Solution and DLS Measurement.** The hydrodynamic diameter and polydispersity of PCP-Dox prodrug and PMEMA-Hyd-Dox was investigated by DLS at 25 °C. The PCP-Dox aqueous solution was prepared by dissolving the prodrug in deionized water, with the final concentration of 1 mg/mL, and stirred overnight in the dark at 25 °C. In addition, the sample of PMEMA-Hyd-Dox was prepared by dialysis method. A total of 4 mg PMEMA-Hyd-Dox was dissolved in 1 mL of DMSO for 1 h, and the solution was added dropwise into 4 mL of deionized water and stirred for another 2 h. Then the resulting solution was dialyzed against deionized water for 12 h to remove DMSO. Before the DLS measurement, the two samples were filtered using 0.45 μm filters to produce a particle-free solution.

**2.12. In Vitro Drug Release.** The release of Dox from PCP-Dox prodrug and PMEMA-Hyd-Dox was examined using a dialysis method against phosphate buffered saline (PBS) at pH 7.4 and 5.0 at 37 °C, respectively. A total of 2 mg PCP-Dox was dissolved in 2 mL of PBS (pH 5.0, 7.4), then transferred to a dialysis bag (MWCO 3500), and immersed in a tube containing 18 mL of PBS (pH 5.0, 7.4) with constant stirring at 37 °C. A 1 mg aliquot of PMEMA-Hyd-Dox was dissolved in 0.1 mL of DMSO and then added dropwise into 2 mL of PBS (pH 5.0, 7.4) with stirring. Finally, the resulting solution was transferred to a dialysis bag (MWCO 3500) and immersed in a tube containing 18 mL of PBS (pH 5.0, 7.4) with constant stirring at 37 °C. At specific time intervals, 0.5 mL of buffer solution outside the dialysis bag was withdrawn and subjected to UV–vis measurements. The same volume of fresh medium was replaced after every measurement. The mass of released Dox was determined on the basis of the UV absorbance intensity at 480 nm for Dox using a standard calibration curve experimentally obtained. The release amount was calculated by eq 1.<sup>14</sup>

$$m_{\text{act}} = \left( C_t + \frac{\nu}{V} \sum_0^{t-1} C_t \right) V \quad (1)$$

where *m<sub>act</sub>* is the actual mass of Dox released at time *t*, *C<sub>t</sub>* is the Dox concentration in release media at time *t*, measured on UV–vis spectrometer, *ν* is the sample volume taken at a fixed time interval, and *V* is the total volume of the solution (20 mL). The experiment was performed in triplicate.

**2.13. Cell Viability Assay.** The cell viability was evaluated by Celltiter-Blue cell viability assay (Premoga Corporation). HepG2, A549, and MCF-7 cells were grown in Dulbecco's modified Eagle's medium (DMEM) with high glucose containing 10% fetal bovine serum (FBS), 100 units per mL of penicillin, and 100 μg/mL of streptomycin at 37 °C in a 5% CO<sub>2</sub> humidified atmosphere. Then cells were seeded in 96-well flat-bottomed plates at a density of 6 × 10<sup>3</sup> cells per well and cultured for 24 h. After that, the medium was replaced by serum-free DMEM containing different concentrations of free Dox, PCP-Dox, and PMEMA-Hyd-Dox. After incubation for 1 h, the medium was removed and washed three times with PBS and then replaced with fresh serum-free DMEM. After further incubation for 47 h, 10 μL of Celltiter-Blue reagent was added to each well, and the plates were incubated for another 4 h at 37 °C. Then, the fluorescence

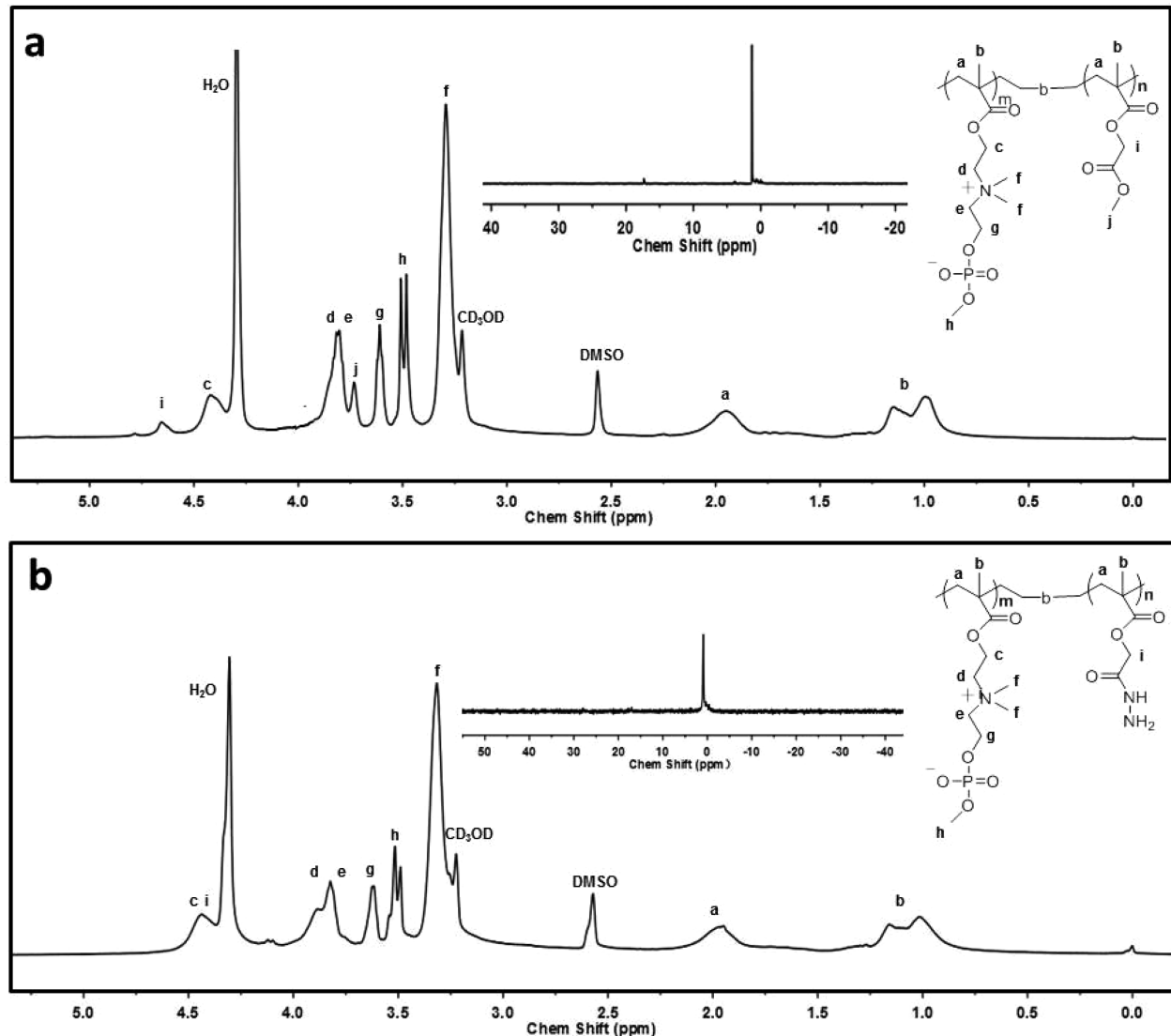


**Figure 2.** (a) <sup>1</sup>H and <sup>31</sup>P NMR spectra of PMCP-*b*-PMEMA; (b) <sup>1</sup>H and <sup>31</sup>P NMR spectra of PMCP-*b*-PMEMA-hydrazide.

signal was measured by microplate reader ( $\lambda_{\text{ex}} = 560 \text{ nm}$ ,  $\lambda_{\text{em}} = 590 \text{ nm}$ ). The experiment was performed in triplicate.

In addition, the cell viability of the polymer precursor (PMCP-*b*-PMEMA-Hydrazide) was evaluated by the same method. HepG2, A549, and MCF-7 cells were seeded in 96-well flat-bottomed plates at a density of  $6 \times 10^3$  cells per well and cultured for 24 h. After that, the medium was replaced by serum-free DMEM containing different concentrations of precursor. After incubation for 48 h, 10  $\mu\text{L}$  of Celltiter-Blue reagent was added to each well, and the plates were incubated for another 4 h at 37 °C. Then, the fluorescence signal was measured by microplate reader ( $\lambda_{\text{ex}} = 560 \text{ nm}$ ,  $\lambda_{\text{em}} = 590 \text{ nm}$ ). The experiment was performed in triplicate. The cell viability was calculated based on the eq 2.

$$\text{cell viability}(\%) = \frac{\text{fluorescent intensity(sample)}}{\text{fluorescent intensity(control)}} \times 100\% \quad (2)$$

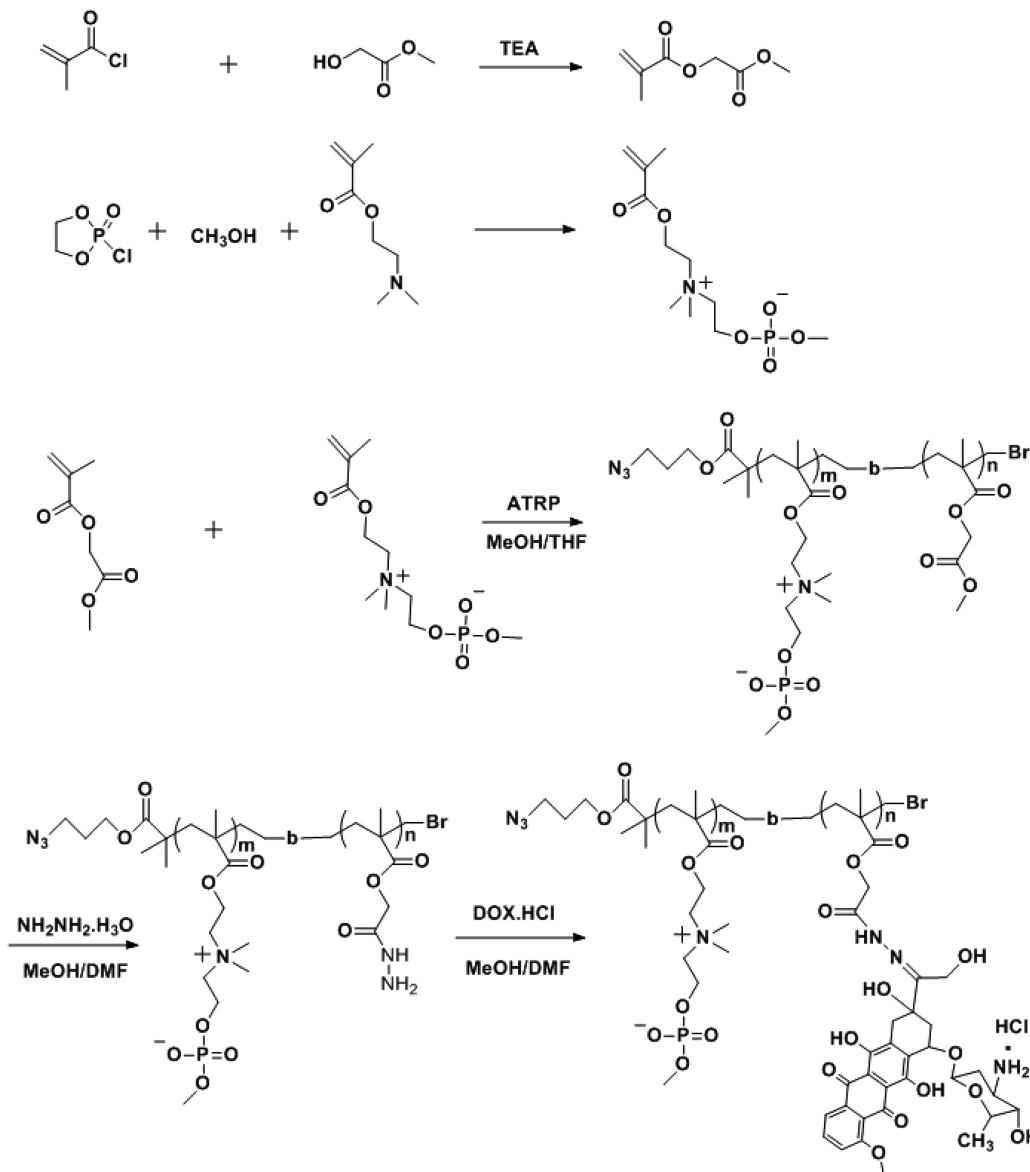
**2.14. Cellular Uptake Assays.** HepG2, A549, and MCF-7 cells were grown in Dulbecco's modified Eagle's medium (DMEM) with high glucose containing 10% fetal bovine serum (FBS), 100 units per mL of penicillin, and 100  $\mu\text{g}/\text{mL}$  of streptomycin at 37 °C. Then cells were seeded into 24-well plates at a density of  $7 \times 10^4$  cells per well and incubated for 24 h. For cellular internalization study, the cells were treated with free Dox, PCP-Dox, and PMEMA-Hyd-Dox in serum-free DMEM for 10, 30, and 60 min, respectively. The original

concentration of Dox in all samples was 10  $\mu\text{g}/\text{mL}$ . After incubation, the cells were washed three times with PBS. Finally, 0.5 mL of serum-free DMEM was added to each well, and the fluorescence images were obtained using confocal laser scanning microscopy. In the process of taking the images, all the camera parameters (laser intensity, image brightness, exposure, magnification, etc.) were fixed.

The fluorescence intensity was determined by flow cytometry. HepG2, A549, and MCF-7 cells were grown in Dulbecco's modified Eagle's medium (DMEM) with high glucose containing 10% fetal bovine serum (FBS), 100 units per mL of penicillin, and 100  $\mu\text{g}/\text{mL}$  of streptomycin at 37 °C. Then cells were seeded into 12-well plates at a density of  $2 \times 10^5$  cells per well and incubated for 24 h. After that, the cells were incubated with serum-free DMEM containing free Dox, prodrug, and PMEMA-Hyd-Dox for 10, 30, and 60 min, respectively. The original concentration of Dox in all samples was 10  $\mu\text{g}/\text{mL}$ . After incubation for a fixed time, the cells were washed three times with PBS, then treated with trypsin, and centrifuged. Finally, the cells were suspended in 0.3 mL of PBS and determined with flow cytometer.

### 3. RESULTS AND DISCUSSION

**3.1. Synthesis of the Polymer Prodrug PCP-Dox.** In our previous works we have demonstrated the CP group could strongly interact with the PC group.<sup>24–28</sup> To optimize the multivalent CP–PC interactions, we synthesized fully func-

Scheme 2. Detailed Synthetic Strategies for PMCP-*b*-PMEMA-Hyd-Dox

tional CP-containing monomer 2-(methacryloyloxy) ethyl choline phosphate (MCP) with the highest CP valency available according to the previous method;<sup>28</sup> the <sup>1</sup>H and <sup>31</sup>P NMR spectra are shown in Figure 1a ( $D_2O$ ) and Figure S1 ( $DMSO-d_6$  and  $CD_3OD$ , 1:1, v/v); we also detected the final purified MCP monomer via electrospray mass spectrometry, and the MS image (Figure S2) showed identification of the mass peaks, at mass to charge ratio (*m/z*) 296.11 atomic mass units ( $M + H$ ) and 318.09 ( $M + Na$ ). Unfortunately, the yield of the MCP monomer was low because this reaction was extremely sensitive to oxygen and moisture. In addition, the side products have similar properties to the MCP monomer, which made the purification of the products get more difficult. Therefore, this reaction should be performed under absolutely anhydrous conditions and the absence of oxygen to minimize the side products, and we get better results (yield: 52%). Meanwhile, a new monomer, 2-methoxy-2-oxoethyl methacrylate (MEMA), was also synthesized. The MEMA was easily synthesized by a one-step condensation reaction between acyl chloride and a hydroxyl group, and the monomer could be

adequately activated by hydrazine hydrate, whose <sup>1</sup>H NMR was shown in Figure 1b. The signals located at  $\delta$  1.9, 5.8, and 6.1 ppm belonged to the protons of methacrylate, and those at  $\delta$  3.7 and 4.8 ppm were attributed to methyl glycolate, indicating the monomer has been synthesized successfully.

Then, the polymer prodrug PCP-Dox ( $PMCP_{40}$ -PMEMA<sub>12</sub>-Hydrazide-Dox, used in all of the next investigations, and <sup>1</sup>H NMR is shown in Figure S5) was synthesized by a multistep reactions, the detailed procedures are shown in Scheme 2. First, the macroinitiator PMEMA-Br (Table 1, 1#), <sup>1</sup>H NMR of which was shown in Figure 1C, was synthesized by ATRP of MEMA using 3-azidopropyl 2-bromo-2-methylpropanoate as an initiator. Then, the block copolymer PMEMA-*b*-PMCP (Table 1, 3#) was synthesized by ATRP using PMEMA-Br (Table 1, 2#) as macroinitiator; the <sup>1</sup>H and <sup>31</sup>P NMR spectra (Figure 2a) indicated the copolymer was successfully synthesized. The signals of a double bond disappeared and the characteristic signals of PMEMA ( $\delta$  3.67) and PMCP ( $\delta$  3.23, 3.44, 3.54, 3.75) can be clearly observed. The polydispersities and  $M_n$  of PMEMA-*b*-PMCP and PMEMA-

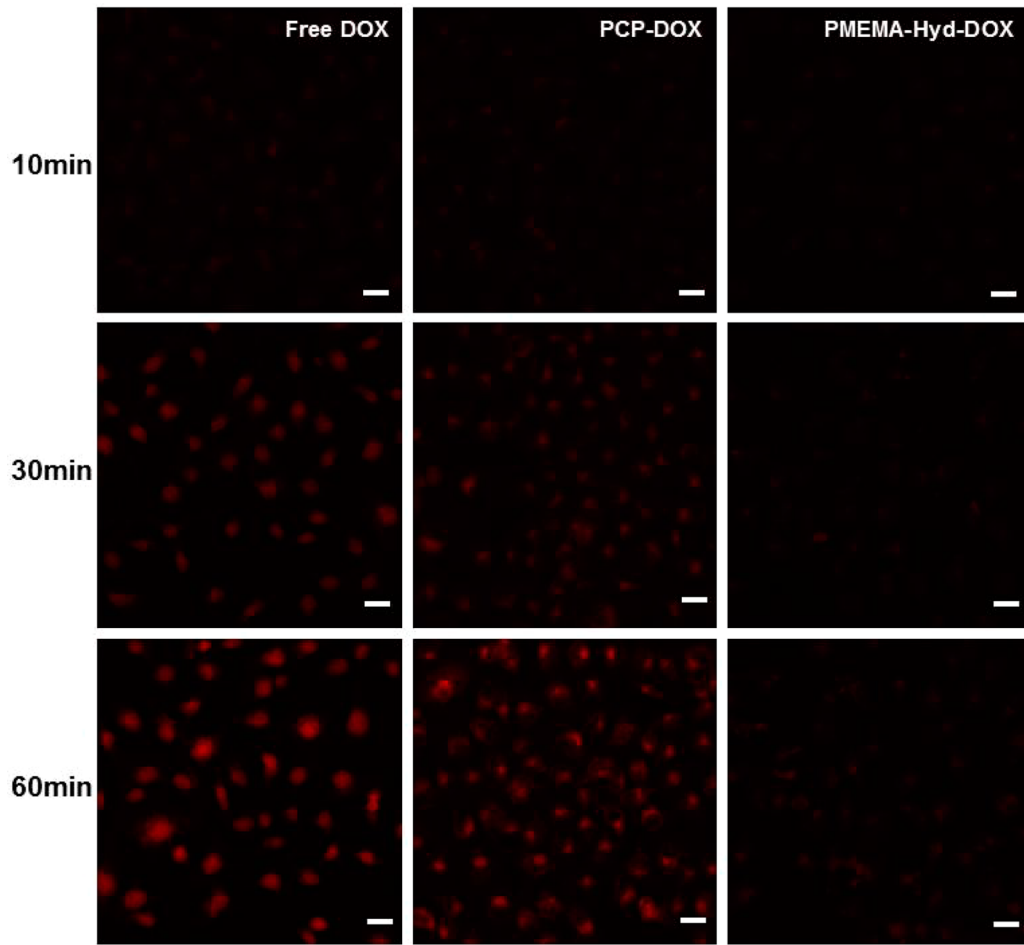


**Figure 3.** Confocal microscopy images of MCF-7 cells treated by free Dox, PCP-Dox prodrug, and the control with equivalent Dox concentration to be 10  $\mu\text{g}/\text{mL}$  for 10, 30, and 60 min. Scale bar: 50  $\mu\text{m}$ .

Br, determined by GPC and  $^1\text{H}$  NMR (as shown in Table 1 and Figure S6) indicated PMEMA-Br had a low polydispersity. The polyCP containing polymers would be retained on the columns when the  $M_n$  and polydispersity of PMEMA-PMCP were measured by GPC, so the  $M_n$  was determined from the  $^1\text{H}$  NMR through comparison of the integrals of the PMEMA ( $\delta$  3.67), PMCP ( $\delta$  3.54), and initiator 3-azidopropyl 2-bromo-2-methylpropanoate ( $\delta$  3.43).

Subsequently, PMCP-*b*-PMEMA-hydrazide was synthesized by hydrazinolysis in the presence of hydrazine hydrate. As the  $^1\text{H}$  NMR (Figure 2b) showed, the characteristic peak  $j$  of PMEMA (-COOCH<sub>3</sub>) disappeared, which demonstrated that the hydrazinolysis of methyl ester groups was complete.<sup>36</sup> After the hydrazinolysis of PMCP-*b*-PMEMA, the anticancer Dox was conjugated to the polymer carrier via acid-labile hydrazone bond using trifluoroacetic acid as catalyst, the loading content of Dox was ~10.0 wt % determined by UV-vis spectroscopy on the basis of the UV absorbance intensity at 480 nm for Dox. Meanwhile, PMEMA-Hyd-Dox (PMEMA<sub>30</sub>-hydrazide-Dox, used in all the next investigations and  $^1\text{H}$  NMR is shown in Figure S4) was synthesized by the same method. The  $^1\text{H}$  NMR of PMEMA-hydrazide (Figure S3) showed the hydrazinolysis of PMEMA was complete, and the Dox content of PMEMA-Hyd-Dox was ~20.0 wt %, indicating a high loading of this anticancer drug.

**3.2. Cellular Uptake Assay of PCP-DOX.** To demonstrate whether prodrug PCP-Dox can be more efficiently internalized

by tumor cells within a short time, we compared the cellular internalization behaviors of free Dox, PCP-Dox, and the control at various cell lines MCF-7, A549, and HepG2. And the cellular internalization efficiency was evaluated by confocal laser scanning microscopy (CLSM) at fixed time interval. The images of MCF-7 cell line were shown in Figure 3 and Figure S8. It can be found that free Dox and PCP-Dox prodrug were remarkably internalized within 10 min, and both of them increased continuously as the extension of incubation time within 1 h. It can be found from the continuous fluorescence images captured within 1 h that the internalization efficiency of PCP-Dox is comparable to that of free Dox. However, after being incubated with PMEMA-Hyd-Dox for 1 h, only weak Dox fluorescence can be observed in the cancer cells. The results indicated the cellular uptake of PCP-Dox was faster and more efficient than the controlled one. The same results were also observed in the other two tumor cell lines, as shown in Figures S9 and S10.

To further confirm PCP-Dox prodrug could be more efficiently internalized by tumor cells, we further detected the fluorescence intensity of the tumor cells incubated with free Dox, PCP-Dox prodrug, and the control using flow cytometry. The cellular internalization efficiency of the Dox by MCF 7 cell line was associated with the fluorescence signals. As shown in Figure 4, free Dox and PCP-Dox polymer prodrug were efficiently uptaken after incubated 10 min, but the fluorescence signal incubated by the control almost overlapped with the

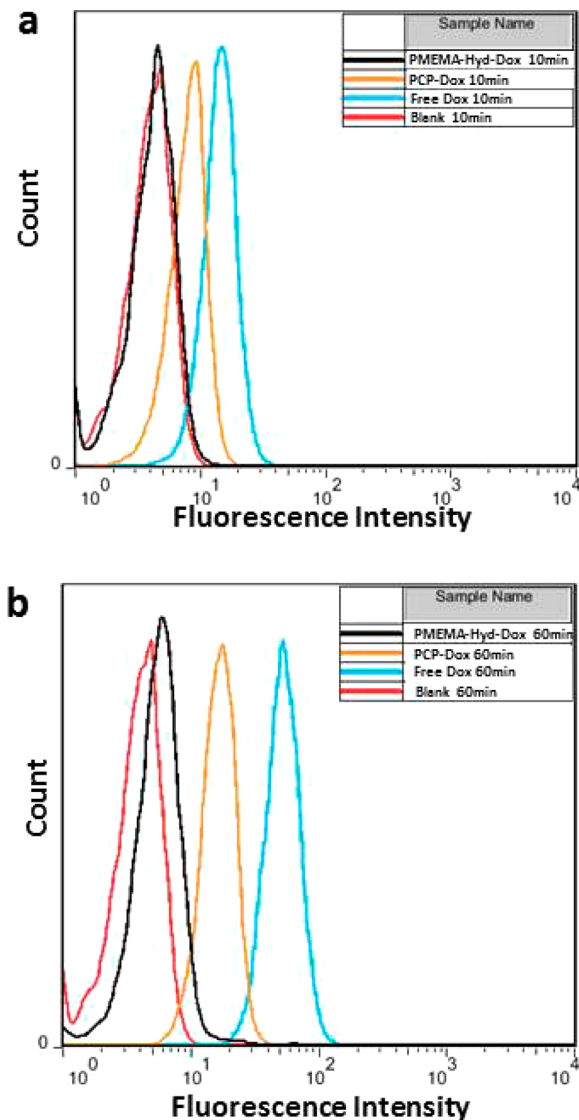


**Figure 4.** Flow cytometry analysis of MCF-7 cells treated by free Dox, PCP-Dox prodrug, and control with equivalent Dox concentration to be  $10 \mu\text{g}/\text{mL}$  for 10 (a) and 60 min (b).

blank, indicating the sluggish and inefficient internalization for the PMEMA-Hyd-Dox. After incubating for 1 h, the fluorescence signal of the cells incubated with free Dox and PCP-Dox prodrug was remarkably larger than that of those incubated with the control. The same results were also observed in other tumor cell lines, as shown in Figures S11 and S12. It can be seen that the results of flow cytometry are consistent with the CLSM results, which all collectively demonstrated PCP-Dox prodrug could be more rapidly and efficiently internalized by various tumor cells within 1 h.

It is well-known that the entrance of free Dox into the cells was accomplished by passive diffusion without requirement for specific transporter and ATP consumption.<sup>37–39</sup> Dox first bind to the cell membrane with anionic PC headgroup via electrostatic interaction, and then is internalized by cells through a flip-flop mechanism between the two membrane leaflets, so the whole process of cellular internalization of free Dox was very fast.<sup>37–39</sup> But for the polymer drug delivery system, endocytosis was the main mechanism for cellular internalization after binding to the membrane.<sup>40,41</sup> It was

troublesome for PMEMA-Hyd-Dox without CP groups to bind to the cell membrane over a short time, and the endocytosis consumed ATP, which lead to the sluggish cellular internalization of PMEMA-Hyd-Dox. However, for PCP-Dox, the strong interactions between CP groups and cell membranes, which accelerated polymer prodrug bind to the cell membrane, and then rapidly internalized into the cell, which largely enhance the efficiency of the internalization of the prodrug. Although the cellular internalization efficiency of the novel prodrug was a little lower than that of free Dox, it increased largely compared with the polymer carrier without CPs and has made significant progress. In addition, the most interesting thing is that this prodrug PCP-Dox is suitable for all kinds of tumor cells instead of some specific cells, and the internalization efficacy are all enhanced when it was applied to various tumor cells, and the prodrug PCP-Dox has more better control and release process compared with free Dox, which suggests that PCPs can be used as a novel carrier to deliver drugs.

**3.3. In Vitro Drug Release and the Size Distribution of the PCP-Dox Prodrug.** As an ideal polymer drug delivery system, the anticancer drug should be rapidly and efficiently released from the carrier upon reaching the target. To promote the release of anticancer drug, Dox was conjugated to the polymer carrier via acid-labile hydrazone bond, which was easily cleaved at acid environment. In order to justify the pH-triggered drug release, in vitro drug release at different pH values were determined. As shown in Figure 5a, only 6.4% Dox was released after the PCP-Dox was incubated at pH 7.4 for 65 h, which indicated that the polymer prodrug was stable under neutral pH environment. The interesting thing is that the release rate of Dox was dramatically accelerated at pH 5.0, which should be attributed to the acidic catalytic cleavage of hydrazone linkage between PMEMA and Dox. It can be seen that within the first 24 h, 32.8% Dox was released from the prodrug, and about 60.0% Dox was released after incubated 65 h. The whole release process was continuous and depended on the hydrolysis kinetics of hydrazone bonds. The results indicated that the Dox loaded by our designed prodrug can be effectively controlled released, and circumvent the rapid “burst” drug release outside of the cancer cells, and the drug release of PMEMA-Hyd-Dox showed the same tendency as PCP-Dox shown in Figure 5a. Meanwhile, DLS measurement showed that the PCP-Dox has a similar size distribution to PMEMA-Hyd-Dox. As shown in Figure 5b, the averaged diameter of the PCP-Dox in aqueous solution was determined to be about 147.1 nm (PDI: 0.244), and the averaged diameter of the PMEMA-Hyd-Dox in aqueous solution was determined to be about 180.3 nm (PDI: 0.175).

**3.4. Cell Viability Assays.** It is widely recognized that an ideal polymeric drug delivery system must be nontoxic. We determined the *vitro* cytotoxicity of the polymer precursor by Celltiter-Blue cell viability assays. We incubated MCF-7, HepG2, and A549 cell lines with different concentrations of polymer precursor for 48 h. It can be found from Figures 6a and S13 that the polymer precursor showed nontoxicity to three tumor cell lines at the concentrations from 12.5 to  $500 \mu\text{g}/\text{mL}$ , demonstrating that PMCP-*b*-PMEMA-hydrazide had low toxicity and good biocompatibility.

To demonstrate the anticancer efficacy of PCP-Dox prodrug, the Celltiter-Blue cell viability assays was also adopted. We incubated MCF-7, HepG2, and A549 cell lines with different concentrations of prodrug for 1 h, then the medium was replaced with fresh serum-free DMEM and incubated for

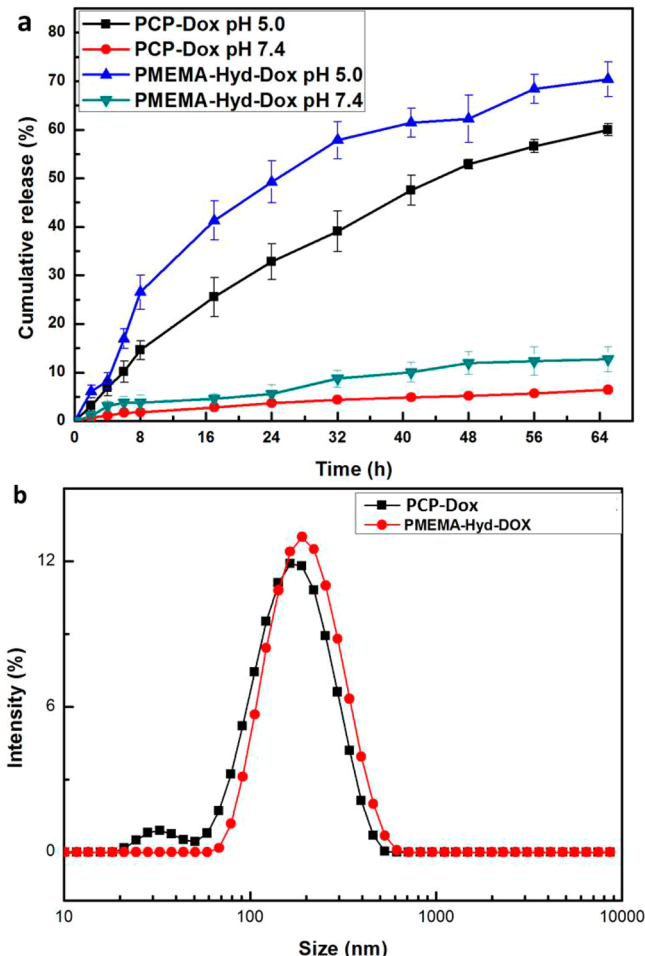


**Figure 5.** (a) In vitro Dox release from the PCP-Dox prodrug and PMEMA-Hyd-Dox in PBS buffer under different pHs (pH 7.4 and 5.0). (b) Size distribution of PCP-Dox prodrug and PMEMA-Hyd-Dox in aqueous solution.

another 47 h. It can be seen from Figures 6b and S14 that the PCP-Dox prodrug showed enhanced cytotoxicity to the three tumor cell lines compared with the PMEMA-Hyd-Dox, which can be attributed to the enhanced cellular internalization for PCP-Dox prodrug within 1 h and efficient release of Dox in cells. Meanwhile, with increasing Dox concentrations from 0.5 to 20  $\mu\text{g}/\text{mL}$ , the cell viability was further decreased. In addition, the cell viability of PCP-Dox prodrug was higher than that of free Dox, which may be because the cellular uptake for free Dox was more efficient than PCP-Dox. On the other hand, the cleavage of the hydrazone linkage between polymer carriers and Dox at endosome/lysosome was time-dependent, which depended on the hydrolysis kinetics of hydrazone bonds. After the Dox cleaved from the polymer carriers, it must escape from the endosome/lysosome and then diffuse into the nucleus to exert their cytostatic effects, which further decreased the *vitro* cytotoxicity of PCP-Dox prodrug compared with free Dox.

#### 4. CONCLUSIONS

In this study, we designed and synthesized a novel polymer-drug conjugate system PCP-Dox. This polymer prodrug decorated with multivalent CP groups can significantly accelerate cell internalization within 1 h via multiple CP-PC quadrupole interaction. Furthermore, the Dox-loaded polymer prodrug exhibited noticeable pH-triggered behavior with Dox

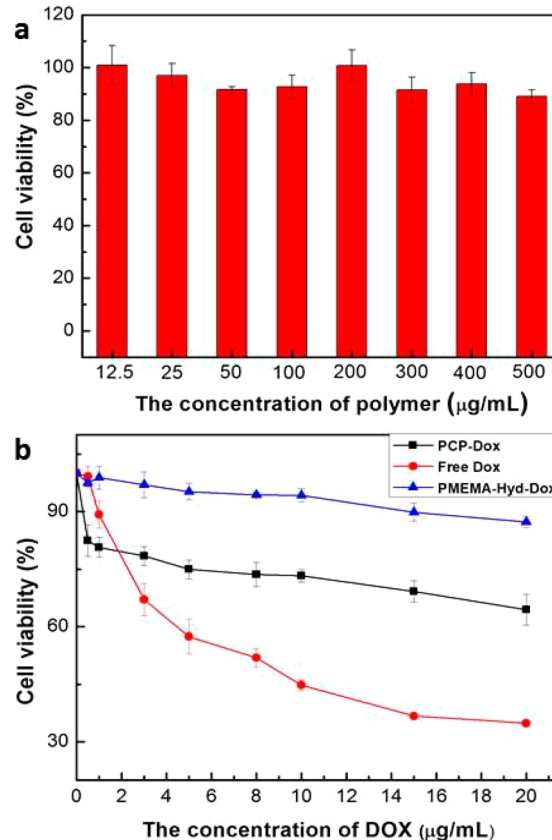


**Figure 6.** (a) Cell viability of MCF-7 cells incubated with various concentrations of the polymer precursor for 48 h; (b) Incubated with different concentrations of free DOX, PCP-Dox prodrug, and control for 1 h, then replaced with fresh serum-free DMEM and incubated for another 47 h.

release through hydrazone bond cleaved under acidic conditions. The *in vitro* cytotoxicity studies showed that polymer precursor had good biocompatibility and low toxicity, but the polymer prodrug showed enhanced cytotoxicity to various tumor cells. It is expected that the as-prepared polymer carriers based on multivalent CP groups can be used as a new drug carriers for targeted delivery with improved cellular internalization efficiency, especially suitable for delivery of the cargo molecules which are unstable in physiological conditions, like nucleic acids, peptides, or proteins.

#### ASSOCIATED CONTENT

##### Supporting Information

The Supporting Information is available free of charge on the ACS Publications website at DOI: [10.1021/acs.biomac.6b00455](https://doi.org/10.1021/acs.biomac.6b00455).

Additional supporting figures ([PDF](#)).

#### AUTHOR INFORMATION

##### Corresponding Authors

\*E-mail: [xjma@ciac.ac.cn](mailto:xjma@ciac.ac.cn).

\*E-mail: [xfyu@ciac.ac.cn](mailto:xfyu@ciac.ac.cn). Tel.: +86 431 85262678.

##### Author Contributions

<sup>§</sup>These authors contributed equally to this work (W.W. and B.W.).

##### Notes

The authors declare no competing financial interest.

## ACKNOWLEDGMENTS

The financial support from the Nation Natural Science Foundation of China (21304096, 21474103) is acknowledged.

## REFERENCES

- (1) Xu; Liu, X.; Liu, T.; Wang, H.; Qian, J. *Mater. Sci. Eng., C* **2015**, *50*, 341–347.
- (2) Furgeson, D. Y.; Dreher, M. R.; Chilkoti, A. *J. Controlled Release* **2006**, *110*, 362–369.
- (3) Liu, C.; Liu, F.; Feng, L.; Li, M.; Zhang, J.; Zhang, N. *Biomaterials* **2013**, *34*, 2547–2564.
- (4) Krakovicova, H.; Etrych, T.; Ulbrich, K. *Eur. J. Pharm. Sci.* **2009**, *37*, 405–412.
- (5) Kostkova, H.; Etrych, T.; Rihova, B.; Kostka, L.; Starovoytova, L.; Kovar, M.; Ulbrich, K. *Macromol. Biosci.* **2013**, *13*, 1648–1660.
- (6) Zhou, Z.; Li, L.; Yang, Y.; Xu, X.; Huang, Y. *Biomaterials* **2014**, *35*, 6622–6635.
- (7) Chen, X.; Parelkar, S. S.; Henchey, E.; Schneider, S.; Emrick, T. *Bioconjugate Chem.* **2012**, *23*, 1753–1763.
- (8) Cui, J.; Yan, Y.; Wang, Y.; Caruso, F. *Adv. Funct. Mater.* **2012**, *22*, 4718–4723.
- (9) Car, A.; Baumann, P.; Duskey, J. T.; Cham, M.; Bruns, N.; Meier, W. *Biomacromolecules* **2014**, *15*, 3235–3245.
- (10) Chen, W.; Zhong, P.; Meng, F.; Cheng, R.; Deng, C.; Feijen, J.; Zhong, Z. *J. Controlled Release* **2013**, *169*, 171–179.
- (11) Zhan, F.; Chen, W.; Wang, Z.; Lu, W.; Cheng, R.; Deng, C.; Meng, F.; Liu, H.; Zhong, Z. *Biomacromolecules* **2011**, *12*, 3612–3620.
- (12) Shirakura, T.; Kelson, T. J.; Ray, A.; Malyarenko, A. E.; Kopelman, R. *ACS Macro Lett.* **2014**, *3*, 602–606.
- (13) Du, J. Z.; Tang, Y. Q.; Lewis, A. L.; Armes, S. P. *J. Am. Chem. Soc.* **2011**, *133*, 17560–17563.
- (14) Xu, Z.; Zhang, K.; Hou, C.; Wang, D.; Liu, X.; Guan, X.; Zhang, X.; Zhang, H. *J. Mater. Chem. B* **2014**, *2*, 3433–3437.
- (15) Hu, X.; Liu, S.; Huang, Y.; Chen, X.; Jing, X. *Biomacromolecules* **2010**, *11*, 2094–2102.
- (16) Huo, M.; Yuan, J.; Tao, L.; Wei, Y. *Polym. Chem.* **2014**, *5*, 1519–1528.
- (17) Greco, F.; Arif, I.; Botting, R.; Fante, C.; Quintieri, L.; Clementi, C.; Schiavon, O.; Pasut, G. *Polym. Chem.* **2013**, *4*, 1600–1609.
- (18) Bertrand, N.; Wu, J.; Xu, X.; Kamaly, N.; Farokhzad, O. C. *Adv. Drug Delivery Rev.* **2014**, *66*, 2–25.
- (19) Chen, W.; Yuan, Y.; Cheng, D.; Chen, J.; Wang, L.; Shuai, X. *Small* **2014**, *10*, 2678–2687.
- (20) Ulbrich, K.; Subr, V. *Adv. Drug Delivery Rev.* **2004**, *56*, 1023–1050.
- (21) Du, J. Z.; Du, X. J.; Mao, C. Q.; Wang, J. *J. Am. Chem. Soc.* **2011**, *133*, 17560–17563.
- (22) Wang, Y.; Wang, Y.; Xiang, J.; Yao, K. *Biomacromolecules* **2010**, *11*, 3531–3538.
- (23) Cheng, C.; Wei, H.; Shi, B. X.; Cheng, H.; Li, C.; Gu, Z. W.; Cheng, S. X.; Zhang, X. Z.; Zhuo, R. X. *Biomaterials* **2008**, *29*, 497–505.
- (24) Yu, X.; Liu, Z.; Janzen, J.; Chafeeva, I.; Horte, S.; Chen, W.; Kainthan, R. K.; Kizhakkedathu, J. N.; Brooks, D. E. *Nat. Mater.* **2012**, *11*, 468–476.
- (25) Yu, X.; Zou, Y.; Horte, S.; Janzen, J.; Kizhakkedathu, J. N.; Brooks, D. E. *Biomacromolecules* **2013**, *14*, 2611–2621.
- (26) Yu, X.; Yang, X.; Horte, S.; Kizhakkedathu, J. N.; Brooks, D. E. *Biomaterials* **2014**, *35*, 278–286.
- (27) Yu, X.; Yang, X.; Horte, S.; Kizhakkedathu, J. N.; Brooks, D. E. *Macromol. Biosci.* **2014**, *14*, 334–339.
- (28) Yu, X.; Yang, X.; Horte, S.; Kizhakkedathu, J. N.; Brooks, D. E. *Chem. Commun.* **2013**, *49*, 6831–6833.
- (29) Hu, G.; Parelkar, S. S.; Emrick, T. *Polym. Chem.* **2015**, *6*, 525–530.
- (30) Hu, G.; Emrick, T. *J. Am. Chem. Soc.* **2016**, *138*, 1828–1831.
- (31) Wang, F.; Liu, J. *J. Am. Chem. Soc.* **2015**, *137*, 11736–11742.
- (32) Chen, X.; Chen, T.; Lin, Z.; Li, X.; Wu, W.; Li, J. *Chem. Commun.* **2015**, *51*, 487–490.
- (33) Li, S. Y.; Liu, L. H.; Jia, H. Z.; Qiu, W. X.; Rong, L.; Cheng, H.; Zhang, X. Z. *Chem. Commun.* **2014**, *50*, 11852–11855.
- (34) Duan, X.; Xiao, J.; Yin, Q.; Zhang, Z.; Yu, H.; Mao, S.; Li, Y. *ACS Nano* **2013**, *7*, 5858–5869.
- (35) Topham, P. D.; Sandon, N.; Read, E. S.; Madsen, J.; Ryan, A. J.; Armes, S. P. *Macromolecules* **2008**, *41*, 9542–9547.
- (36) Wang, H.; Xu, F.; Li, D.; Liu, X.; Jin, Q.; Ji, J. *Polym. Chem.* **2013**, *4*, 2004–2010.
- (37) Krylova, O. O.; Melik-Nubarov, N. S.; Badun, G. A.; Ksenofontov, A. L.; Menger, F. M.; Yaroslavov, A. A. *Chem. - Eur. J.* **2003**, *9*, 3930–3936.
- (38) Regev, R.; Eytan, G. D. *Biochem. Pharmacol.* **1997**, *54*, 1151–1158.
- (39) Regev, R.; Yeheskely-Hayon, D.; Katzir, H.; Eytan, G. D. *Biochem. Pharmacol.* **2005**, *70*, 161–169.
- (40) Nam, H. Y.; Kwon, S. M.; Chung, H.; Lee, S.-Y.; Kwon, S.-H.; Jeon, H.; Kim, Y.; Park, J. H.; Kim, J.; Her, S.; Oh, Y.-K.; Kwon, I. C.; Kim, K.; Jeong, S. Y. *J. Controlled Release* **2009**, *135*, 259–267.
- (41) Hillaireau, H.; Couvreur, P. *Cell. Mol. Life Sci.* **2009**, *66*, 2873–2896.